Dispersion-managed soliton in a strong dispersion map limit

P. M. Lushnikov

Theoretical Division, Los Alamos National Laboratory, MS-B284, Los Alamos, New Mexico 87545, and Landau Institute for Theoretical Physics, Kosygin Street 2, Moscow 117334, Russia

Received March 12, 2001

A dispersion-managed optical system with stepwise periodic variation of dispersion is studied in a strong dispersion map limit in the framework of the path-averaged Gabitov–Turitsyn equation. The soliton solution is obtained by analytical and numerical iteration of the path-averaged equation. An efficient numerical algorithm for finding a DM soliton shape is developed. The envelope of soliton oscillating tails is found to decay exponentially in time, and the oscillations are described by a quadratic law.

OCIS codes: 060.2330, 060.5530, 060.4370, 190.5530, 260.2030.

A dispersion-managed[1] (DM) optical system is designed to create low (or even zero) path-averaged dispersion by periodic alternation of the dispersion sign along an optical fiber, which dramatically reduces pulse broadening. Recently, dispersion management has become an essential technology for development of ultrafast high-bit-rate optical communication lines.[2–8] The lossless propagation of an optical pulse in a DM fiber is described by a nonlinear Schrödinger equation with periodically varying dispersion $d(z)$:

$$iu_z + d(z)u_{tt} + |u|^2 u = 0\,, \tag{1}$$

where u is the pulse envelope, z is the propagation distance, and all quantities are made dimensionless. Consider a two-step periodic dispersion map: $d(z) = \langle d\rangle + \tilde{d}(z)$, where $\tilde{d}(z) = d_1$ for $0 < z + nL < L_1$ and $\tilde{d}(z) = d_2$ for $L_1 < z + nL < L$; $L \equiv L_1 + L_2$ is a dispersion map period; $\langle d\rangle$ is the path-averaged dispersion; d_1 and d_2 are the amplitudes of dispersion variation subject to the condition that $d_1 L_1 + d_2 L_2 \equiv 0$; and n is an arbitrary integer number.

A nonlinearity can be treated as a small perturbation on a scale of dispersion map period L, provided that the characteristic nonlinear length $Z_{\rm nl}$ of the pulse is large: $Z_{\rm nl} \gg L$, where $Z_{\rm nl} = 1/|p|^2$ and p is a typical pulse amplitude. Then, Eq. (1) is reduced to a path-averaged Gabitov–Turitsyn model[4]:

$$i\hat{\psi}_z(\omega) - \omega^2\langle d\rangle\hat{\psi} + R(\hat{\psi}, \omega) = 0\,, \tag{2}$$

where

$$R(\hat{\psi}, \omega) = \frac{1}{(2\pi)^2}\int \frac{\sin s\Delta/2}{s\Delta/2}\,\hat{\psi}(\omega_1)\hat{\psi}(\omega_2) \times \hat{\psi}^*(\omega_3)\delta(\omega_1 + \omega_2 - \omega_3 - \omega)\mathrm{d}\omega_1\mathrm{d}\omega_2\mathrm{d}\omega_3\,, \tag{3}$$

$\Delta \equiv {\omega_1}^2 + {\omega_2}^2 - {\omega_3}^2 - \omega^2$, $s = d_1 L_1$ is the dispersion map strength, $\hat{\psi} \equiv \hat{u}\exp[i\omega^2\int_{L_1/2}^{z}\tilde{d}(z')\mathrm{d}z']$ is a slow function of z on a scale L, and $\hat{\psi}(\omega) = \int_{-\infty}^{\infty}\psi(t)\exp(i\omega t)\mathrm{d}t$ is a Fourier component of ψ. The Gabitov–Turitsyn model is well supported by numerical simulations.[8,9]

Considering the DM soliton $\psi = A(t)\exp(i\lambda z)$ (A is real) of Gabitov–Turitsyn equation (2) and then returning to t space, one gets[9]

$$-\lambda A + \langle d\rangle A_{tt} = \frac{1}{2\pi s}\int Ci(t_1 t_2/s)A(t_1 + t) \times A(t_2 + t)A(t_1 + t_2 + t)\mathrm{d}t_1\mathrm{d}t_2\,, \tag{4}$$

where $Ci(x) = \int_{\infty}^{x}\cos x/x\mathrm{d}x$. It was found numerically[3] that the Gaussian ansatz,

$$A_{\rm Gauss} = p\exp\!\left(-\frac{\beta}{2}\,t^2\right), \tag{5}$$

where p and β are real constants, is a rather good approximation of the DM soliton solution. Thus one can effectively use Eq. (5) as a zero approximation for solving Eq. (4) by iterations, as was done in Ref. 10 for $\langle d\rangle = 0$. Following Ref. 10, one can make a generalization for the case of small but nonzero average dispersion, $|d_0| \ll |d_1|$, and obtain the following expression by substitution of zero the iteration (5) into the nonlinear term in Eq. (4) and integration over ω_1, ω_2:

$$-\lambda A_{\rm Gauss} + \langle d\rangle(A_{\rm Gauss})_{tt} + \frac{p^3}{2\tilde{s}}\int_{-\tilde{s}}^{\tilde{s}}\frac{\exp\!\left(-\dfrac{\beta}{2}\,\dfrac{3i + s'}{i + 3s'}\,t^2\right)}{(1 - 2is' + 3s'^2)^{1/2}}\,\mathrm{d}s' = A_{\rm corr}\,, \tag{6}$$

where $\tilde{s} \equiv \beta s$ and $A_{\rm corr}$ represents correction from higher-order iterations. Neglecting $A_{\rm corr}$ and series expanding Eq. (6) in powers of t^2, one can get a set of two transcendental equations from the zero- and first-order terms of this expansion. The respective equations are

$$\lambda = -\beta\langle d\rangle + \frac{p^2}{2\sqrt{3}\,\tilde{s}}\left(\operatorname{arcsinh}\frac{3\tilde{s} - i}{2} + \text{c.c.}\right),$$
$$\lambda = -3\beta\langle d\rangle + \frac{2p^2}{3\tilde{s}}\left[\left(\frac{\tilde{s} + i}{3\tilde{s} - i}\right)^{1/2} + \frac{\sqrt{3}}{12}\operatorname{arcsinh}\frac{3\tilde{s} - i}{2} + \text{c.c.}\right], \tag{7}$$

where c.c. means complex conjugation. Equations (7) form a closed set of equations for determining the parameters β and p of Gaussian ansatz (5) for each value of λ and s.

0146-9592/01/201535-03$15.00/0

The solution of Eq. (4) was also obtained by numerical iteration. The $n+1$th iteration, $A^{(n+1)}$, is given by

$$\hat{A}^{(n+1)}(\omega) = Q_n^{3/2} \frac{R[\hat{A}^{(n)}, \omega] + (|\langle d\rangle| - \langle d\rangle)\omega^2 \hat{A}^{(n)}(\omega)}{\lambda + |\langle d\rangle|\omega^2}, \tag{8}$$

where the functional $R(\hat{A}, \omega)$ is defined in Eq. (3), Q_n is a stabilizing factor given by

$$Q_n = \left. \frac{\hat{F}^{-1}\left[\dfrac{\lambda + \langle d\rangle\omega^2}{\lambda + |\langle d\rangle|\omega^2}\hat{A}^{(n)}(\omega)\right]}{\hat{F}^{-1}\left[\dfrac{R(\hat{A}, \omega)}{\lambda + |\langle d\rangle|\omega^2}\right]} \right|_{t=0}, \tag{9}$$

and $\hat{F}^{-1}$ is a backward Fourier transform. A similar numerical iteration scheme was also used in the study reported in Ref. 11, except that a Petviashvili stabilizing factor[12] was used instead of Q_n. However, the use of both stabilizing factors results in the convergence of iteration scheme to the same solution of Eq. (4).

The main obstacle in the numerical iteration scheme [Eqs. (8) and (9)] is the computation of integral term $R(\hat{A}, \omega)$, which generally requires N^3 operations for each iteration, where N is a number of grid points in ω or t space. Here a much more efficient numerical algorithm for calculation of $R(\hat{A}, \omega)$ is introduced.

Rewriting the kernel of $R(\hat{\psi}, \omega)$ as

$$\frac{\sin s\Delta/2}{s\Delta/2} = \frac{1}{s}\int_{-s/2}^{s/2} \exp(is'\Delta)\mathrm{d}s', \tag{10}$$

and using the definition of Δ, one gets from Eq. (3)

$$R(\hat{A}, \omega) = \frac{1}{s(2\pi)^2}\int_{-s/2}^{s/2} \mathrm{d}s' \exp(-is'\omega^2)\int \hat{A}^{(s')}(\omega_1) \times \hat{A}^{(s')}(\omega_2)\hat{A}^{(s')*}(\omega_3)\delta(\omega_1 + \omega_2 - \omega_3 - \omega)\mathrm{d}\omega_1\mathrm{d}\omega_2\mathrm{d}\omega_3, \tag{11}$$

where $\hat{A}^{(s')}(\omega) \equiv \hat{A}(\omega)\exp(is'\omega^2)$. In t space, Eq. (11) takes the form

$$\hat{F}^{-1}[R(\hat{A}, \omega)] = \frac{1}{s}\int_{-s/2}^{s/2} \mathrm{d}s' \mathbf{G}^{(s')}[\Psi^{(s')}(t)], \tag{12}$$

where $\Psi^{(s')}(t) \equiv |A^{(s')}(t)|^2 A^{(s')}(t)$ and $\mathbf{G}^{(s')}$ is an integral operator corresponding to a multiplication operator $\hat{\mathbf{G}}^{(s')}[\hat{\Psi}^{(s')}(\omega)] \equiv \exp(-is'\omega^2)\hat{\Psi}(s')$ in ω space. It follows from Eqs. (11) and (12) that the numerical procedure for calculation of $R(\hat{A}, \omega)$ includes four steps: (i) The backward Fourier transform of $\hat{A}^{(s')}(\omega) = \hat{A}(\omega)\exp(is'\omega^2)$ for every value of s'. (ii) A calculation of $\Psi^{(s')}(t)$ from $A^{(s')}(t)$. (iii) The forward Fourier transform of $\Psi^{(s')}(t)$. (iv) A numerical integration (summation) of $\exp(-is'\omega^2)\hat{\Psi}^{(s')}(\omega)$ over s' for every value of ω. A fast Fourier transform requires $N\log_2(N)$ operations. The total number of operations for one iteration is $\sim 2MN\log_2(N)$, where M is a number of grid points for integration over s'. The typical values for numerical solution of Eq. (4) were $N = 2048$ and $M = 800$. One iteration on an Alpha 500 MHz workstation requires ~ 10 s for 16-byte (32-digit) precision. Thus, the numerical scheme (i)–(iv) dramatically improves numerical performance. 2048^3 operations would take 10 h on the same workstation. Note that one can generalize the proposed efficient numerical algorithm to include fiber losses and amplifiers.

Figure 1 shows the dependence of a rms pulse width, $T_{\mathrm{RMS}} \equiv (\int t^2 A^2 \mathrm{d}t / \int A^2 \mathrm{d}t)^{1/2}$, on quasi-momentum λ obtained from (i) the first iteration of Eq. (4) with values of β and p obtained from Eqs. (7) (dotted curves); (ii) a variational approach [see, e.g., Eqs. (13) and (14) in Ref. 11 and the references in that paper] represented by dashed curves; (iii) a full numerical solution of Eq. (4) (solid curves). The explicit expression $T_{\mathrm{RMS}} = 1/\sqrt{2\beta}$ for the Gaussian pulse shape is used for calculation of the dashed curves. The solid curve in Fig. 1(b) represents only upper branch I of the solution because the numerical iteration scheme for negative average dispersion $\langle d\rangle = -0.01$ diverges on lower branch II, which is in agreement with Ref. 11. A time-averaged optical power $P \equiv \int A^2 \mathrm{d}t$ was also calculated, and it was found that $P(\lambda)$ dependence following from the first iteration and the variational approach[11] reproduce a full numerical solution of Eq. (4) with high accuracy ($\sim$1 error%). One can conclude that both Eqs. (7) and the variational approach[11] predict $P(\lambda)$ with high accuracy, whereas $T_{\mathrm{RMS}}(\lambda)$ dependence is reproduced by the first iteration of Eq. (4) with better accuracy ($\sim$2 error%) than that of the variational approach ($\sim$40%).

There is an essential difference between the present numerical simulation and the numerical results of

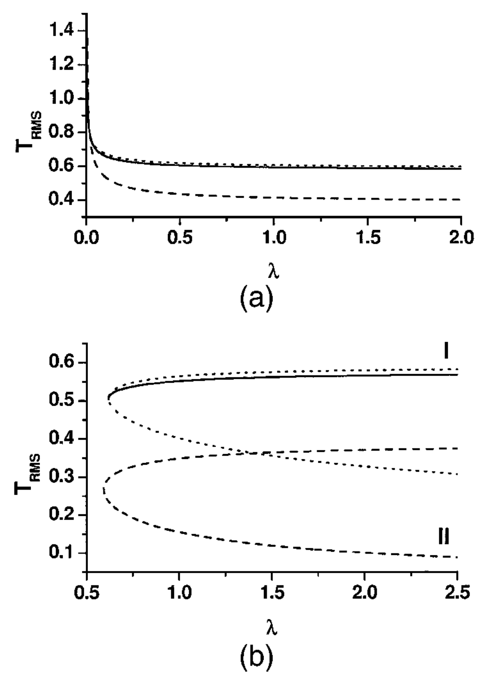

Fig. 1. T_{RMS} for (a) $s = 1$, $\langle d\rangle = 0.01$ and (b) $\langle d\rangle = -0.01$. Branches I and II for $\langle d\rangle = -0.01$ correspond to two branches of the analytical solution.

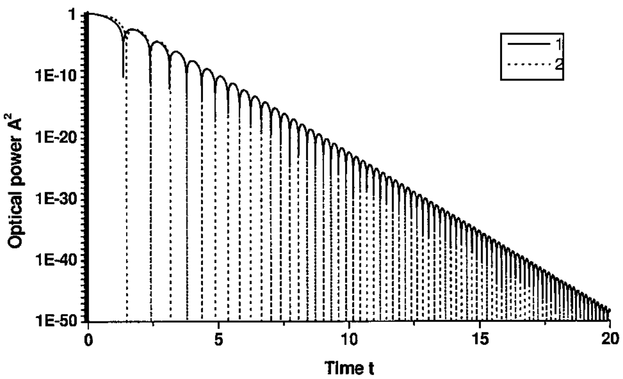

Fig. 2. DM soliton shape (curve 1) versus Eq. (11) (curve 2) for $\langle d \rangle = 0$, $s = 1$, and $\lambda = 1$. $A(t)$ is an even function.

Ref. 11 concerning upper branch I for the negative average dispersion. After ~50 iterations of Eq. (4), a numerical instability was detected in the tails of the DM soliton for $\langle d \rangle = -0.01$. Presumably this instability was not found in the study reported in Ref. 11 because only a few iterations were considered there. Another reason is that Q_n is an integral quantity, and the growth of numerical instability in the tails of the DM soliton makes an exponentially small contribution to Q_n. Thus Q_n is not a good parameter for detection of fine details of iteration convergence of DM soliton tails. A finer numerical grid slows down numerical instability growth but does not stop it. The instability slow down as $\langle d \rangle \to 0$, and for $\langle d \rangle \geq 0$ there is no numerical instability. Thus the solid curve in Fig. 1(b) for $\langle d \rangle = -0.01$ can be formally attributed to the DM soliton, and the question about the existence of a DM soliton for the negative average dispersion is still open. It is possible that the instability within the numerical iteration scheme results from a resonance of DM soliton tails with linear waves.[11] However, there is another alternative, that the DM soliton solution does not exist for any negative average dispersion value and that instead of a DM soliton one can observe a long-lived quasi-stable structure. Note that the existence of the DM soliton of Eq. (4) for nonnegative average dispersion was proved in Ref. 13. In addition, it was proved in Ref. 14 that, even if a DM soliton exists for $\langle d \rangle < 0$, the DM soliton cannot realize a minimum of the Hamiltonian of Eq. (2) for fixed P, indicating that the DM soliton is unstable. A related result[15] is the nonexistence criterion for a periodic solution of the Eq. (1) for a negative enough average dispersion. However, Refs. 13–15 do not give any statement about the existence of a DM soliton for small negative $\langle d \rangle$.

Figure 2 shows a typical DM soliton shape. This is, to the best of my knowledge, the first high-precision numerical solution of Eq. (4). Note that the solid curve's dips do not reach the t axes only because of the finite size of the numerical grid. One can conjecture from Fig. 2 that the asymptote of the DM soliton is given by

$$A_{\mathrm{asymp}}(t) = f(t)\cos\{t^2[a_0 + a(t)]\}\exp(-b|t|)\,, \qquad (13)$$

where a_0 and b are constants and $f(t)/|t|$ and $a(t)$ are slow functions of t. An analysis of fast oscillations in the integral term of Eq. (4) makes it possible to show that $f(t) = c|t| + O(1)$, $a_0 = 1/(2s)$, and $a(t) = a_1/|t| + a_2/t^2 + O(1/|t|^3)$ for $|t| \to \infty$, $\langle d \rangle \to 0$, where c, a_1, and a_2 are real constants. The dashed curve in Fig. 2 shows the $A^2_{\mathrm{asymp}}(t)$ dependence of $c = 11.9654$, $b = 3.04515$, $a_1 = 1.41364$, and $a_2 = 1.51023$, which is in very good agreement with the asymptote of the numerical solution of Eq. (4) (solid curve). Thus the envelope of the DM soliton's oscillating tails decays exponentially, and the oscillations are described by a quadratic law. Note that asymptotic solution (13) includes a dependence on $|t|$, which is nonanalytic at $t = 0$, and thus this solution cannot be extended to $t = 0$. Instead, Eq. (13) needs to be matched with the approximate solution obtained from Eq. (6), which is valid for small t. Also, it should be mentioned that asymptotic solution (13) differs strongly from the asymptote of the first iteration given by Eq. (12) of Ref. 10. This result indicates that the first iteration is a good approximation of the DM soliton solution only for small t. Detailed consideration of the asymptotic solution is outside the scope of this Letter.

The author thanks M. Chertkov, I. R. Gabitov, E. A. Kuznetsov, and V. Zharnitsky for helpful discussions. Support was provided by the U.S. Department of Energy (contract W-7405-ENG36), the Russian Foundation for Basic Research (RFBR; grant 00-01-00929). The author's e-mail address is lushnikov@cnls.lanl.gov.

References

1. C. Lin, H. Kogelnik, and L. G. Cohen, Opt. Lett. **5,** 476 (1980).
2. M. Nakazawa and H. Kubota, Electron. Lett. **31,** 216 (1995).
3. N. J. Smith, F. M. Knox, N. J. Doran, K. J. Blow, and I. Bennion, Electron. Lett. **32,** 54 (1996).
4. I. Gabitov and S. K. Turitsyn, Opt. Lett. **21,** 327 (1996).
5. S. Kumar and A. Hasegawa, Opt. Lett. **22,** 372 (1997).
6. T. Lakoba and D. J. Kaup, Electron. Lett. **34,** 1124 (1998).
7. L. F. Mollenauer, P. V. Mamyshev, J. Gripp, M. J. Neubelt, N. Mamysheva, L. Grüner-Nielsen, and T. Veng, Opt. Lett. **25,** 704 (2000).
8. S. K. Turitsyn, T. Schäfer, N. J. Doran, K. H. Spatschek, and V. K. Mezentsev, Opt. Commun. **163,** 122 (1999).
9. M. J. Ablowitz and G. Biondini, Opt. Lett. **23,** 1668 (1998).
10. P. M. Lushnikov, Opt. Lett. **25,** 1144 (2000).
11. D. E. Pelinovsky, Phys. Rev. E **62,** 4283 (2000).
12. V. I. Petviashvili and O. A. Pokhotelov, *Solitary Waves in Plasmas and in the Atmosphere* (Gordon & Breach, Philadelphia, Pa., 1992), p. 248.
13. V. Zharnitsky, E. Grenier, S. K. Turitsyn, C. K. R. T. Jones, and J. S. Hesthaven, Phys. Rev. E **62,** 7358 (2000).
14. V. Zharnitsky, E. Grenier, C. K. R. T. Jones, and S. K. Turitsyn, Physica D **152,** 794 (2001).
15. P. M. Lushnikov, JETP Lett. **72,** 111 (2000).